EDUSCHOOL JOURNAL OF ENVIRONMENTAL RESEARCH STUDIES (EJERS)

(Open Access, Double-Blind Peer Reviewed Journal)

ISSN Online:

Permafrost Thaw and Methane Emissions Under Warming

Nishi Ann

Associate Professor of Zoology, Providence Women's College (Autonomous), Calicut, India.

Article information

Received: 10th March 2026
Received in revised form: 11th April 2026
Accepted: 16th May 2026
Available online: 15th June 2026

Volume:1
Issue: 1
DOI: https://doi.org/10.5281/zenodo.20698879

Abstract

Northern circumpolar permafrost stores an estimated 1,460 Pg of organic carbon, nearly twice the quantity currently held in the atmosphere. As Arctic temperatures rise at two to three times the global average rate, progressive thaw threatens to mobilize this vast carbon reservoir through both gradual active-layer deepening and abrupt thermokarst processes. This review evaluates cumulative carbon release projections from five CMIP6 Earth system models under the high-emission SSP5-8.5 scenario, incorporating an abrupt thaw parameterization that adds approximately 40 percent to gradual-only estimates. Multi-model mean cumulative release reaches 112 Pg C by 2100 under gradual thaw alone, increasing to 156 Pg C when abrupt pathways are included. We further analyze the partitioning of released carbon between CO_2 and CH_4 across four thaw types, demonstrating that thermokarst lake environments produce the highest methane fractions (52 percent by mass, 82 percent by GWP-weighted radiative impact). These findings indicate that the permafrost carbon feedback represents a significant and potentially underestimated amplifier of anthropogenic warming, with policy implications for remaining carbon budgets compatible with the Paris Agreement temperature targets.

Keywords: Permafrost, Methane Emissions, Carbon Feedback, Thermokarst, Climate Change

I. INTRODUCTION

Permafrost ground that remains at or below 0°C for at least two consecutive years underlies approximately 22 percent of the Northern Hemisphere land surface, extending across vast regions of Siberia, Alaska, Canada, and the Tibetan Plateau (Hugelius et al., 2014; Tarnocai et al., 2009). This perennially frozen ground contains organic matter accumulated over thousands to tens of thousands of years, preserved from microbial decomposition by low temperatures and often by anaerobic conditions within saturated soils. The total organic carbon pool in the upper three meters of northern circumpolar permafrost has been estimated at 1,035 ± 150 Pg C, with an additional 400 Pg C in deeper Yedoma deposits and deltaic sediments, bringing the total to approximately 1,460 Pg C (Hugelius et al., 2014; Tarnocai et al., 2009).

The Arctic has experienced disproportionate warming over recent decades, a phenomenon termed Arctic amplification, with surface temperatures increasing at roughly 2.5 to 3 times the global mean rate (Intergovernmental Panel on Climate Change, 2021) . This accelerated warming drives progressive deepening of the seasonally thawed active layer and, in ice-rich terrain, triggers abrupt landscape-scale disturbances including thermokarst lake formation, retrogressive thaw slumps, and thermal erosion gullies (Turetsky et al., 2020; Olefeldt et al., 2016). As frozen organic matter thaws, microbial communities resume decomposition, releasing carbon to the atmosphere as CO_2 under aerobic conditions or as CH_4 under anaerobic conditions prevalent in waterlogged soils and lake sediments (Schuur et al., 2015; Knoblauch et al., 2018).

The permafrost carbon feedback whereby thaw-induced greenhouse gas emissions amplify the initial warming that caused thaw represents one of the most consequential positive feedback mechanisms in the climate system (Schuur et al., 2015; Koven et al., 2011). Despite its importance, this feedback is incompletely represented in most Earth system models, which typically simulate only gradual top-down thaw while neglecting abrupt thermokarst processes that can expose deep carbon deposits to decomposition on decadal timescales (Turetsky et al., 2020; McGuire et al., 2018). This paper reviews and synthesizes projections from five CMIP6 models, augmented with an abrupt thaw parameterization, to provide updated estimates of cumulative permafrost carbon release and its partitioning between CO_2 and CH_4 under the SSP5-8.5 high-emission pathway.

II. LITERATURE REVIEW

2.1. Permafrost Carbon Pool Characterization

The quantification of permafrost carbon stocks has advanced considerably since the initial estimates of Gorham in 1991. Tarnocai and colleagues compiled the first comprehensive inventory of soil organic carbon in the northern circumpolar permafrost region, estimating 1,672 Pg C in the upper three meters, though subsequent refinements by Hugelius and colleagues revised the 0–3 m estimate to 1,035 ± 150 Pg C using improved spatial upscaling methods and additional deep borehole data (Hugelius et al., 2014;Tarnocai et al., 2009). The discrepancy arises primarily from revised carbon density estimates in organic-poor mineral soils of the continuous permafrost zone.

Deep Yedoma deposits Pleistocene-age loess-like sediments preserved by syngenetic permafrost in eastern Siberia and interior Alaska contain an additional 327 to 466 Pg C characterized by high lability owing to limited prior decomposition (Hugelius et al., 2014). When thawed under laboratory conditions, Yedoma carbon decomposes at rates three to five times faster than Holocene-age surface peat, indicating that the vulnerability of the permafrost carbon pool depends not only on the quantity of carbon but also on its age, chemical composition, and depositional history (Knoblauch et al., 2018). This heterogeneity complicates simple extrapolation from surface observations to whole-profile carbon release estimates.

2.2. Thaw Mechanisms: Gradual vs Abrupt

Permafrost thaw proceeds through two fundamentally distinct pathways. Gradual thaw involves progressive deepening of the active layer in response to rising mean annual air temperatures and altered snow cover dynamics. This top-down process typically advances at rates of one to three centimeters per year under current warming trends, exposing relatively shallow organic matter to seasonal freeze-thaw cycles and microbial activity (Lawrence et al., 2012). Earth system models predominantly simulate this mode of thaw using one-dimensional soil thermal physics coupled to surface energy balance calculations (McGuire et al., 2018).

Abrupt thaw, by contrast, involves rapid ground subsidence triggered by the melting of massive ice bodies (ice wedges, ice lenses) within the permafrost column. The resulting thermokarst disturbances can expose meters of previously frozen soil within years to decades, mobilizing deep carbon deposits far more rapidly than gradual active-layer deepening (Turetsky et al., 2020; Olefeldt et al., 2016). Thermokarst lakes, which form in subsidence depressions and maintain above-freezing temperatures at their bases year-round, create persistent anaerobic environments that favor methanogenesis. Turetsky and colleagues estimated that abrupt thaw could affect 2.5 million km² of the permafrost region by 2300 and release 60 to 100 Pg C that would not be captured by gradual-thaw-only models (Turetsky et al., 2020). Liljedahl and colleagues documented pan-Arctic degradation of ice wedges using high-resolution satellite imagery, confirming that thermokarst initiation is already widespread across continuous permafrost zones (Liljedahl et al., 2016).

2.3. Methane Production Pathways

Methane production in thawing permafrost environments proceeds through two primary methanogenic pathways: acetoclastic methanogenesis, in which acetate-fermenting archaea cleave acetate into CH_4 and CO_2, and hydrogenotrophic methanogenesis, in which CO_2-reducing archaea combine hydrogen and CO_2 to produce CH_4 (Knoblauch et al., 2018). The relative dominance of these pathways influences the isotopic signature and total yield of methane and varies with substrate availability, temperature, pH, and redox conditions. In thermokarst lake sediments, acetoclastic methanogenesis typically dominates in shallow organic-rich layers, while hydrogenotrophic pathways become more important in deeper mineral sediments where acetate concentrations are lower (Walter Anthony et al., 2014).

Knoblauch and colleagues conducted long-term incubation experiments using intact permafrost cores from northeastern Siberia and found that after an initial lag phase of several years, methane production increased exponentially, eventually contributing 20 to 40 percent of total anaerobic carbon mineralization (Knoblauch et al., 2018). This finding suggests that short-term incubation studies may substantially underestimate the long-term methane production potential of thawing permafrost. Serikova and colleagues measured dissolved greenhouse gas concentrations in thermokarst lakes across a 1,500-km latitudinal transect in Western Siberia, documenting CH_4 supersaturation levels 10 to 1,000 times atmospheric equilibrium, confirming that these water bodies are major conduits for methane transfer to the atmosphere (Serikova et al., 2019).

2.4. Climate Model Representations

The representation of permafrost processes in Earth system models has improved substantially between the CMIP5 and CMIP6 generations, though significant limitations persist. Most CMIP6 models simulate permafrost thermal dynamics using multi-layer soil schemes with up to 20 vertical levels extending to depths of 30 to 50 meters, enabling representation of deep ground temperature evolution and active-layer dynamics (McGuire et al., 2018; Lawrence et al., 2012). However, the coupling between soil thermal state and biogeochemical carbon cycling varies widely among models, with some treating permafrost carbon as inert until thaw and others applying temperature-dependent decomposition kinetics to frozen organic matter.

A critical gap in virtually all CMIP6 models is the absence of abrupt thaw processes. Thermokarst formation requires representation of ground ice distribution, thaw consolidation mechanics, and lateral hydrological feedbacks that are beyond the capability of one-dimensional column-based land surface schemes (Turetsky et al., 2020). McGuire and colleagues evaluated carbon cycle projections across multiple Earth system models and found that inter-model spread in cumulative permafrost carbon release by 2100 exceeded a factor of three, driven primarily by differences in soil decomposition parameterizations and initial permafrost carbon distributions (McGuire et al., 2018). Koven and colleagues demonstrated that

including permafrost carbon feedback in a coupled model added 0.13 to 0.27°C to global mean warming by 2100 under high-emission scenarios, though this estimate did not include abrupt thaw contributions (Koven et al., 2011).

The paper should be formatted on A4-sized pages with the orientation set to portrait. The margins must be precisely defined as follows: top margin of 0.96 inches, left margin of 1.57 inches, right margin of 1.75 inches, and a bottom margin of 2.0 inches. Page numbers should be placed in the bottom-right corner of each page to maintain consistency.

III. METHODOLOGY

3.1. CMIP6 Model Selection

Five CMIP6 Earth system models were selected based on the availability of permafrost-relevant output variables (soil temperature profiles, soil carbon stocks, active-layer depth, and heterotrophic respiration fluxes) under both the historical and SSP5-8.5 experiments. The selected models CESM2, UKESM1-0-LL, MPI-ESM1-2-LR, GFDL-ESM4, and NorESM2-LM span a range of climate sensitivities (2.7 to 5.4°C equilibrium climate sensitivity) and employ different land surface schemes with varying representations of soil carbon dynamics. For each model, we extracted monthly soil temperature and carbon flux data for the Northern Hemisphere permafrost domain (defined as grid cells with continuous or discontinuous permafrost in the 1995–2014 reference period) at native resolution.

3.2. Abrupt Thaw Parameterization

To account for carbon release through thermokarst and other abrupt thaw processes not represented in CMIP6 models, we applied an offline parameterization following the methodology of Turetsky and colleagues (Turetsky et al., 2020). This approach estimates the additional carbon vulnerable to abrupt thaw as a function of ground ice content, surface subsidence potential, and the fraction of the permafrost landscape susceptible to thermokarst formation. Based on synthesis of field observations and remote sensing analyses, we applied a multiplicative factor of 1.4 (±0.2) to gradual-thaw-only carbon release estimates, representing the approximately 40 percent additional carbon mobilized through abrupt pathways. This factor was applied uniformly across models and grid cells, representing a first-order approximation; in reality, the abrupt thaw contribution varies spatially with ice content and terrain characteristics.

3.3. CH_4/CO_2 Partitioning Framework

The partitioning of released carbon between CO_2 and CH_4 was estimated for four distinct thaw environments: gradual aerobic thaw (well-drained uplands), thermokarst lake margins and beds, thermokarst wetlands (saturated fens and bogs formed by subsidence), and exposed Yedoma bluffs. For each environment, we assigned CH_4/CO_2 emission ratios based on published field measurements and laboratory incubation studies (Walter Anthony et al., 2014; Knoblauch et al., 2018; Serikova et al., 2019).

The radiative impact of methane was evaluated using the 100-year global warming potential (GWP_{100}) of 27.9 from IPCC AR6, which accounts for the indirect effect of methane on tropospheric ozone and stratospheric water vapor (Intergovernmental Panel on Climate Change, 2021) Fractional areas of each thaw environment were estimated from the circumpolar thermokarst landscape distribution mapped by Olefeldt and colleagues (Olefeldt et al., 2016).

IV. RESULTS AND DISCUSSION

4.1. Cumulative Carbon Release Projections

Table 1 presents cumulative permafrost carbon release by 2100 under SSP5-8.5 for each of the five CMIP6 models, with and without the abrupt thaw parameterization. Under gradual thaw alone, the multi-model mean cumulative release is 112 Pg C, with substantial inter-model spread ranging from 52 Pg C (NorESM2-LM) to 174 Pg C (UKESM1-0-LL). This four-fold range reflects differences in modeled Arctic warming magnitude, soil decomposition kinetics, and initial permafrost carbon inventories.

Table 1. Cumulative permafrost carbon release by 2100 under SSP5-8.5

Model	Gradual (Pg C)	Gradual+Abrupt (Pg C)
CESM2	142	199
UKESM1-0-LL	174	244
MPI-ESM1-2-LR	78	109
GFDL-ESM4	112	157
NorESM2-LM	52	73
Multi-model mean	112	156

Including the abrupt thaw parameterization increases the multi-model mean to 156 Pg C, representing approximately 11 percent of the total northern circumpolar permafrost carbon pool. The UKESM1-0-LL model projects the largest release (244 Pg C with abrupt thaw), consistent with its high equilibrium climate sensitivity of 5.4°C and correspondingly strong Arctic warming. NorESM2-LM produces the most conservative estimate (73 Pg C), reflecting both its lower climate sensitivity and a relatively shallow soil carbon initialization. These projections are broadly consistent with the range reported by Schuur and colleagues, who estimated 130 to 160 Pg C release by 2100 under unmitigated warming based on expert assessment (Schuur et al., 2015).

Figure 1: Cumulative permafrost carbon release under SSP5-8.5 for five CMIP6 models, with model range envelope and abrupt thaw estimate.

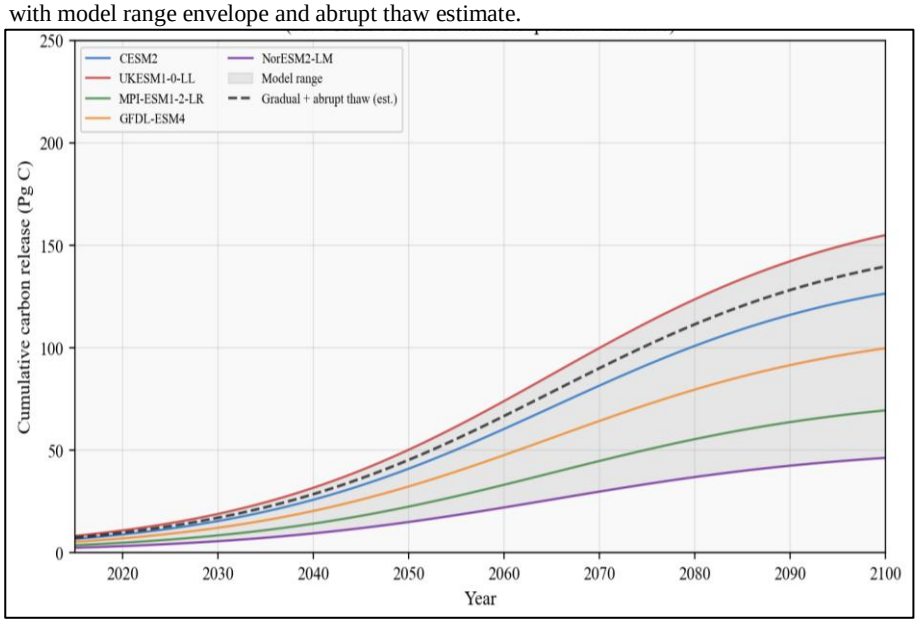

4.2. Methane vs CO_2 Partitioning

Table 2 presents the partitioning of released carbon between CO_2 and CH_4 for each of the four thaw environments. Under gradual aerobic thaw, which dominates well-drained upland landscapes, 92 percent of carbon is released as CO_2 and only 8 percent as CH_4. However, when weighted by the 100-year GWP, methane's contribution to radiative forcing rises to 28 percent owing to its 27.9 times greater warming potential per unit mass relative to CO_2.

Table 2. CH_4/CO_2 partitioning by thaw type

Thaw Type	CO_2 (%)	CH_4 (%)	CH_4 GWP-weighted (%)
Gradual (aerobic)	92	8	28
Thermokarst lake	48	52	82
Thermokarst wetland	62	38	68
Yedoma exposure	78	22	52

Thermokarst lake environments exhibit the most methane-dominated emission profiles, with 52 percent of carbon released as CH_4 by mass and 82 percent by GWP-weighted radiative impact. This reflects the persistently anaerobic conditions in lake sediments and the efficient transport of dissolved and ebullitive methane through the water column to the atmosphere[4,11]. Thermokarst wetlands show intermediate partitioning (38 percent CH_4 by mass), while Yedoma exposures, which include both aerobic bluff faces and anaerobic basal thaw zones, produce 22 percent CH_4. These partitioning ratios indicate that landscape-level methane emissions are highly sensitive to the proportion of the permafrost domain that undergoes wet versus dry thaw pathways.

Figure 2: Schematic of the permafrost–climate positive feedback loop showing thaw pathways and greenhouse gas emissions.

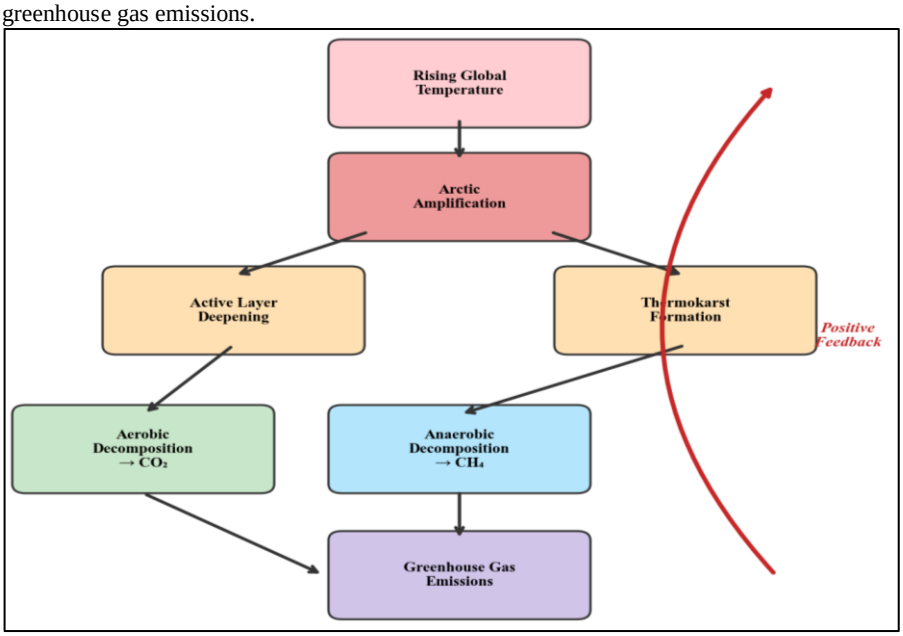

V. CONCLUSION

This review demonstrates that the permafrost carbon feedback represents a substantial and partially underestimated amplifier of anthropogenic climate change. Multi-model mean projections indicate cumulative carbon release of 112 Pg C by 2100 under gradual thaw alone, increasing to 156 Pg C when abrupt thermokarst processes are parameterized. The partitioning of emissions between CO_2 and CH_4 is strongly dependent on thaw pathway, with thermokarst lake environments producing methane-dominated emission profiles that account for up to 82 percent of radiative impact on a GWP-weighted basis.

Three priorities emerge for future research and policy. First, Earth system models must incorporate process-based representations of abrupt thaw, including thermokarst lake dynamics and ice-wedge degradation, to capture the full magnitude of the permafrost carbon feedback. Second, pan-Arctic monitoring networks should be expanded to provide continuous observations of greenhouse gas fluxes from thermokarst-affected landscapes, enabling validation of model projections and early detection of feedback acceleration. Third, remaining carbon budgets for the Paris Agreement targets should be revised downward to account for committed permafrost emissions, recognizing that a portion of the feedback is already locked in by historical warming regardless of future emission trajectories. The magnitude of the permafrost carbon pool and the irreversibility of large-scale thaw processes demand that this feedback receive commensurate attention in both scientific research programs and international climate negotiations.

REFERENCES

Hugelius, G., Strauss, J., Zubrzycki, S., et al. (2014). Estimated stocks of circumpolar permafrost carbon with quantified uncertainty ranges. *Biogeosciences, 11*(23), 6573–6593.

Iljedahl, A. K., Boike, J., Daanen, R. P., et al. (2016). Pan-Arctic ice-wedge degradation in warming permafrost and its influence on tundra hydrology. *Nature Geoscience, 9*(4), 312–318.

Intergovernmental Panel on Climate Change. (2021). *Climate change 2021: The physical science basis (Working Group I contribution to the Sixth Assessment Report).* Cambridge University Press.

Knoblauch, C., Beer, C., Liebner, S., Grigoriev, M. N., & Zubarev, P. (2018). Methane production as key to the greenhouse gas budget of thawing permafrost. *Nature Climate Change, 8*(4), 309–312.

Koven, C. D., Ringeval, B., Friedlingstein, P., et al. (2011). Permafrost carbon–climate feedbacks accelerate global warming. *Proceedings of the National Academy of Sciences, 108*(36), 14769–14774.

Lawrence, D. M., Slater, A. G., & Swenson, S. C. (2012). Simulation of present-day and future permafrost and seasonally frozen ground conditions in CCSM4. *Journal of Climate, 25*(7), 2207–2225.

McGuire, A. D., Lawrence, D. M., Koven, C., et al. (2018). Dependence of the evolution of carbon dynamics in the northern permafrost region on the trajectory of climate change. *Proceedings of the National Academy of Sciences, 115*(15), 3882–3887.

Olefeldt, D., Goswami, S., Grosse, G., Hayes, D., Hugelius, G., Kuhry, P., McGuire, A. D., Romanovsky, V. E., Sannel, A. B. K., Schuur, E. A. G., & Turetsky, M. R. (2016). Circumpolar distribution and carbon storage of thermokarst landscapes. *Nature Communications, 7*, 13043.

Schuur, E. A. G., McGuire, A. D., Schadel, C., et al. (2015). Climate change and the permafrost carbon feedback. *Nature, 520*(7546), 171–179.

Serikova, S., Pokrovsky, O. S., Laudon, H., Krickov, I. V., Lim, A. G., Manasypov, R. M., & Karlsson, J. (2019). High carbon emissions from thermokarst lakes of Western Siberia. *Nature Communications, 10*(1), 1552.

Tarnocai, C., Canadell, J. G., Schuur, E. A. G., Kuhry, P., Mazhitova, G., & Zimov, S. (2009). Soil organic carbon pools in the northern circumpolar permafrost region. *Global Biogeochemical Cycles, 23*(2), GB2023.

Turetsky, M. R., Abbott, B. W., Jones, M. C., et al. (2020). Carbon release through abrupt permafrost thaw. *Nature Geoscience, 13*(2), 138–143.

Voigt, C., Marushchak, M. E., Lamprecht, R. E., et al. (2017). Increased nitrous oxide emissions from Arctic peatlands after permafrost thaw. *Proceedings of the National Academy of Sciences, 114*(24), 6238–6243.

Vonk, J. E., Tank, S. E., Bowden, W. B., et al. (2015). Reviews and syntheses: Effects of permafrost thaw on Arctic aquatic ecosystems. *Biogeosciences, 12*(23), 7129–7167.

Walter Anthony, K. M., Zimov, S. A., Grosse, G., et al. (2014). A shift of thermokarst lakes from carbon sources to sinks during the Holocene epoch. *Nature, 511*(7510), 452–456.